

ENVIRONMENTAL RESEARCH
LETTERS

LETTER

OPEN ACCESS

RECEIVED
12 September 2022REVISED
2 March 2023ACCEPTED FOR PUBLICATION
30 March 2023PUBLISHED
10 May 2023

Original content from
this work may be used
under the terms of the
[Creative Commons
Attribution 4.0 licence](#).

Any further distribution
of this work must
maintain attribution to
the author(s) and the title
of the work, journal
citation and DOI.

Satellite-derived forest canopy greenness shows differential
drought vulnerability of secondary forests compared to primary
forests in PeruBrian R Zutta^{1,*}, Norma Salinas² , Eric G Cosio² , Richard Tito² , Susan Aragón² , Alex Nina-Quispe²
and Rosa Maria Roman-Cuesta^{3,4} ¹ Green Blue Solutions, Lima, Peru² Institute for Nature, Earth and Energy (INTE), Pontificia Universidad Católica del Perú (PUCP), Av. Universitaria 1801, Lima 15088, Peru³ Florence School of Regulation, European University Institute, Florence 50133, Italy⁴ Laboratory of Geoinformation Science and Remote Sensing, University of Wageningen, PO Box 476700AA, Wageningen, The Netherlands

* Author to whom any correspondence should be addressed.

E-mail: bzutta@greenbluesolutions.com**Keywords:** nature climate solutions, tropical forest greenness, secondary forests, drought, evapotranspiration, land surface temperature, climate responseSupplementary material for this article is available [online](#)

Abstract

Understanding tropical secondary forest canopy greenness and responses to climatic conditions is important for climate change mitigation, particularly in the tropics where secondary forest growth is a substantial carbon sink and a promoted natural climate solution. We here test three hypotheses: (a) forest canopy greenness is higher in younger, secondary forests than in older, primary or mature forests, (b) secondary forests are more vulnerable to climatic pressures and (c) there are significant differences between forest types regarding primary–secondary canopy greenness and their differential responses to drought anomalies. To explore these relationships, we monitored wet and dry seasonal greenness from 2001 to 2020, estimated through the enhanced vegetation index (EVI), of Peruvian tropical dry, montane and lowland secondary forests and compared it to nearby primary forests. We developed predictive models of seasonal EVI using remotely sensed variables, including land surface temperature (LST), evapotranspiration (ET), potential evapotranspiration (PET), ratio of ET and PET (ETn), and the standard precipitation index (SPI). Overall, there was a higher change in annual and seasonal EVI for secondary forests compared to primary forests. However, primary forests maintained relatively stable EVI levels during the wet season despite drought anomalies. When decoupling forest type canopy greenness and drought response, primary forest greenness in dry and lowland ecosystems were temporally more stable. Secondary montane had a lower increase in greenness when drought anomalies held during different seasons. Stepwise multiple linear regression models indicated that LST and ETn, a plant water use index, were the most significant factors to predict greening fluctuations in dry and montane forest types. ET and SPI mostly drove wet season mean EVI across all forest types. Predictors of dry season mean EVI varied, but mostly including water availability. Our results suggest that tropical secondary forests are more productive overall yet more vulnerable to prolonged drought.

1. Introduction

With recent increased international focus on climate change, the potential of biomass recovery has led secondary forests to become an important natural

climate solution (Griscom *et al* 2017, 2020) for climate change mitigation, as studies suggest that large amounts of carbon are sequestered during their recovery towards mature forests (Martin *et al* 2013, Chazdon *et al* 2016, Tyukavina *et al* 2017). Tropical

secondary forests may take up CO₂ at 11 times the rate of old-growth forests (Poorter *et al* 2016), with carbon stocks recovering within 40 years of forest regeneration and aboveground carbon stocks possibly increasing past 100 years (Jones *et al* 2019). Therefore, tropical secondary forests seem to be generally very productive and resilient, particularly those with older successional tree species, and driven mainly by variation of water availability, including higher rainfall and lower water deficits, which increases overall biomass growth (Toledo *et al* 2011, Poorter *et al* 2016). However, the opposite response has also been found, where secondary forests seem vulnerable to climate variations with relatively lower carbon balance and growth rates compared to primary forests during dry periods (Elias *et al* 2020, Aragón *et al* 2021).

While these associations are increasingly being studied, knowledge gaps remain in the response of different tropical secondary forest systems to changes in water availability. The well documented Amazon wide moderate and severe drought events occurring in 2005, 2010 and 2015–2016 were linked to strong El Niño Southern Oscillation and North Atlantic sea surface temperature anomalies (Saatchi *et al* 2013, Jiménez-Muñoz *et al* 2016). The 2005 and 2010 drought events were particularly significant, as large areas of Amazonian forests seemed to experience persistent negative effects on forest canopy cover (Saatchi *et al* 2013, Yang *et al* 2018). However, these studies did not focus on local drought anomalies, decouple forest type or explore the impact to neighboring forest ecosystems, which would be useful in understanding the secondary forest's sensitivity.

Satellite observations of a forest's upper canopy characteristics (e.g. greenness) have proven useful to provide the data necessary to observe the long-term impacts of drought (Nakagawa *et al* 2000), with certain limitations due to atmospheric conditions (Saatchi *et al* 2013). Nevertheless, optical indices, in particular the normalized difference vegetation index (NDVI) and the enhanced vegetation index (EVI), are used extensively to estimate vegetation growth and vigor (Wagner *et al* 2017, Potapov *et al* 2021). In particular, the seasonal dynamics of EVI show a sensitive response to droughts throughout the breadth of forest types in the Amazon biome including lowland and montane forests (Costa *et al* 2022, Souza *et al* 2022). In addition, changes in land surface temperature (LST), derived from MODIS and Landsat thermal bands, have been used to predict tropical forest leaf flush and, therefore onset of growth (Brando *et al* 2010). Evapotranspiration (ET) is also a frequent remotely sensed variable, with a long record, used to monitor the overall water cycle, seasonality, and the resulting changes from deforestation in the Amazon (Paca *et al* 2019).

In this study, we tested three hypotheses: (a) forest canopy greenness is higher in younger, secondary

forests compared to older, primary or mature forests, (b) canopy greenness in secondary forests is more vulnerable to climatic pressures than primary forests and (c) there are significant differences between forest types regarding primary–secondary forest canopy greenness and their differential responses to drought anomalies. To this end, we leveraged 20 years of satellite derived data and analyzed spectral data, namely EVI, to identify and understand the greenness response of secondary forests, from different tropical forest ecosystems in Peru, to changes in water availability. We explored the correlation and predictive relationship between the seasonal spectral greenness of secondary forests and nearby primary or mature forests and environmental and climate variables, including LST, ET, and the standard precipitation index (SPI) within the wet and dry seasons.

2. Materials and methods

2.1. Study area

Three different secondary forest types were used for this study: tropical dry forest, tropical lowland rainforest and tropical montane forest (figure 1). One-hectare plots were established in each of the secondary forest sites, all being 30 year old successions. The secondary dry forest site is located in the department of Piura in northern Peru (figure 1(b)), in the protected communal reserve of Manga-Manguilla, in an area known as Tumberos (Tum I, II) (−5.29 °S, −79.85 °W and −5.30 °S, −79.85 °W, respectively). At an elevation of 360–430 m, our sites have an average annual rainfall of 421 mm, with a strong rainfall seasonality from January to April (ca. 90% of the total rainfall). Mean annual temperatures range from 23.5 °C to 25 °C. The forest has been protected since the 90s after intense selective logging for timber occurred. The entire protected area (3000 ha) is dominated by the deciduous tree species *Bursera graveolens* (70% of abundance), with minor contribution from other deciduous genera (e.g. *Loxopterygium*, *Eriotheca*). As a primary control, we selected a one-hectare plot polygon through the visual interpretation of very high spatial resolution satellite imagery in a 5 km-radius area from the secondary plot, at the same elevation and aspect (see next section). While data for the primary forest selected with remote sensing is not available, research under publication for secondary and primary dry plots in the region showed that precipitation largely drives deciduousness with primary dry forests under similar conditions showing deciduousness, but poor species overlapping due to human disturbance legacies (fire, fuel removal, logging) and high levels of endemism. However, some genera from the regional primary plots overlapped (e.g. *Bursera*,

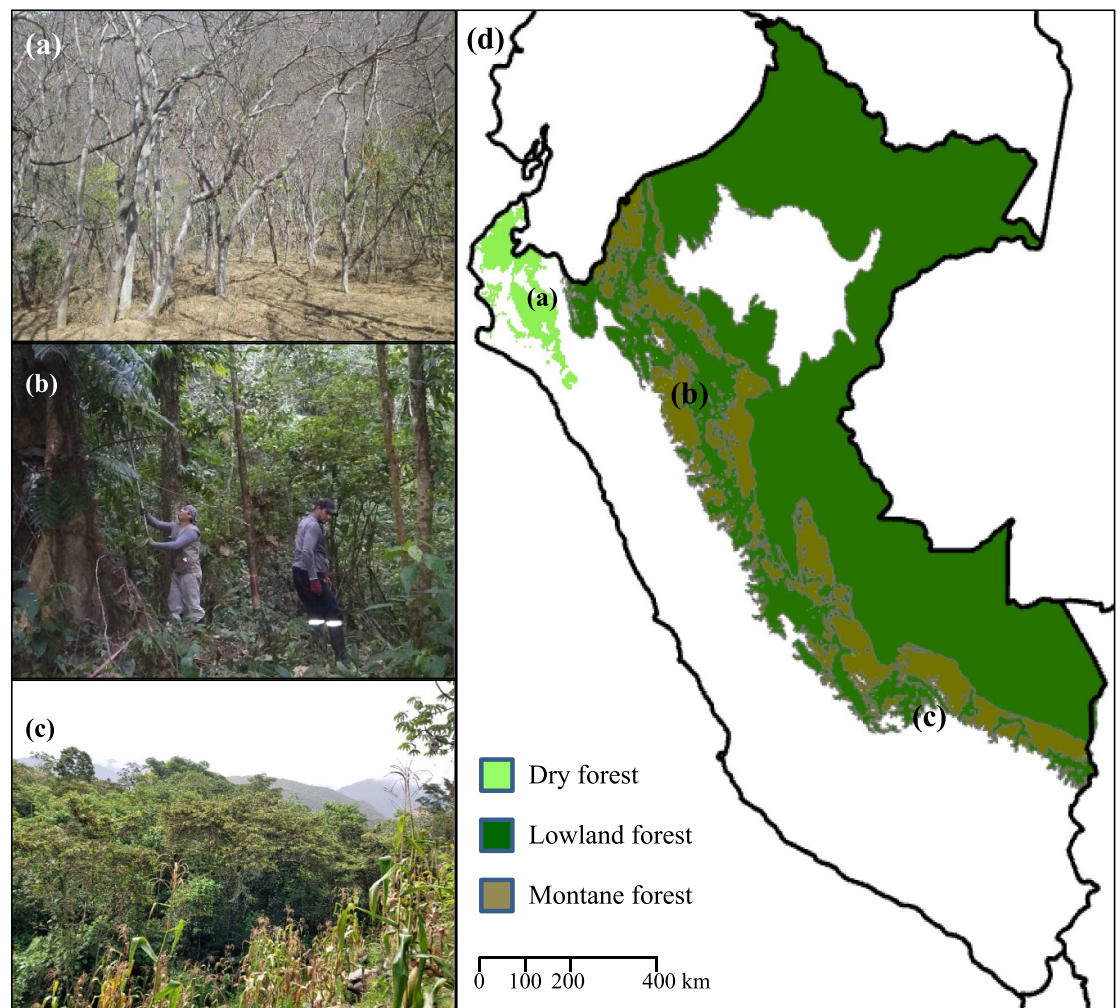


Figure 1. Secondary forest field sites in the (a) tropical dry forest, (b) lowland forest and (c) montane forest within Peru (d).

Loxopterygium, *Handroanthus*, *Eriotheca*) and phenology remains comparable. Structurally, our secondary forests presented mean heights similar to regional primary forests of 9 m, suggesting good phenological and structural comparability among EVIs. No emergent trees were present.

Two secondary lowland rainforest sites were established: one in the Juanjui region, in the department of San Martín in central Peru, in a communal area known as Breo II at ca. 400 m.a.s.l. (-7.15°S , -77.10°W ; figure 1(b)). The rainy season is from October to April with an annual average of 1650 mm and a mean annual temperature of 26.7°C – 28.1°C . An additional secondary site was established in Los Amigos reserve (Ami-I) in the Madre de Dios region of Southern Peru (-12.56°S , -70.10°W) at 250 m.a.s.l. with mean annual rainfall of 2648 mm, and moderate rainfall seasonality (Oct–May being the rainiest months), with 23°C of annual mean temperature. Two primary forest plots were used for comparison in nearby sites (Breo I, -77.16°S , -70.10°W , in Juanjui, but at a higher location 700 masl) and the Tambopata reserve (Tam-9), in Madre de Dios

(-12.83°S , -69.28°W), with similar rainfall. Temperature being fresher in Breo I with mean annual temperatures of 24.3°C – 26.8°C .

Secondary sites in the lowlands have suffered from selective logging (more intensively in Los Amigos than in Juanjui, the latter being an area of harder geographical access) (Salinas pers. com). Both secondary sites present mixed evergreen species with remarkable diversity in Juanjui's Breo II (ca. 60 genera including palms), which is a hotspot of biodiversity and endemism. Most abundant genera in Breo II included: *Inga*, *Hyeronima*, *Apeiba*, *Iryanthera*, *Socratea*, *Otoba*, *Alchornea*, *Marila*, *Matisia*, *Guarea* accounting for 50% of the diversity (Salinas pers. com). Forest diversity in the nearby primary plot (Breo I) was slightly higher with ca. 65 tree genera, and overlapping abundance: *Inga*, *Guatteria*, *Alchornea*, *Apeiba*, *Cecropia*, *Eschweilera*, *Dendropanax*, *Iryanthera*, *Neea*. Structurally, both plots are very similar, mean heights of about 13.7 m and ca. 6% of the trees with diameter at breast height (DBH) >25 cm. Total stems per hectare of ca. 650 trees. Emergent trees with heights >30 m were present in

both plots from evergreen species such as *Sterculia* sp., *Dipteryx* sp., *Myroxylum balsamum*, *Brosimum* sp., *Parkia* sp., *Caryocar* sp., *Clarisia* sp., *Tachigali* sp. A few species of deciduous emergent trees were also present (*Cavanillesia*, *Sterculia*) in both sites but with negligible abundance.

Los Amigos secondary plot hosts ca. 51 genera of evergreen trees and palms with *Pourouma*, *Inga*, *Cecropia*, *Pouteria*, *Pseudolmedia*, *Tachigali*, *Brosimum*, *Jacaranda*, *Meliosma* representing 50% of the abundance (Salinas pers. com). The primary forest of Tambopata showed the highest diversity with 110 evergreen genera. Structurally both primary and secondary were however similar, with mean heights ca. 16 m and mean DBH of ca. 20 cm. Both sites presented ca. 20% of the trees with large trees DBH > 25 cm but Tambopata had more stems ($n = 663$) than Los Amigos ($n = 527$). Emergent trees were all evergreen with species overlap between Tambopata: *Terminalia Amazonia*; *Bertholletia excelsa*; *Jacaranda copaia*; *Brosimum lactescens*; *Ficus indet*; *Acacia indet*; *Sapium marmieri*; *Guatteria pteropus*; *Pourouma minor* and Los Amigos: *Brosimum*, *Acacia*, *Hevea*, *Pseudolmedia*, *Clarisia*, *Inga*, *Hymenaea*, *Tachigali*, *Annona*.

The secondary tropical montane forest was located in the La Convención province, Cusco region, in southern Peru (-12.99°S , -72.53°W ; figure 1(c)) at an elevation of 1700 masl, in a site known as Yanayaco. Annual rainfall averages 1060 mm, with a rainy season from October to April, and a mean annual temperature of 18.4°C (Aragón et al 2021). The one-hectare secondary plot was established on a 30 year abandoned tea plantation and therefore highly disturbed (Aragón et al 2021). All species were evergreen at the secondary plot. Diversity was relatively low (32 genera of trees) with an abundance of agroforestry species (tea, *Eriobotrya japonica*) tea shading genera: *Inga* and *Ocotea* and early succession soft-wood genera like *Cecropia*, *Ficus* and *Urera*. Some primary genera were also present and overlapped with the selected montane control plot (e.g. *Clethra*). Aragón et al (2021) presented a comparison with primary montane plots at similar conditions (1880 m.a.s.l.) from Trocha Union, Cusco region. The plots showed that while all species were evergreen, there was poor genera overlapping due to hard access and high endemism in the Trocha Union region (e.g. *Cyathea*, *Myrcia*, *Tapirira*, *Alzatea*, *Clethra*). Structurally, secondary Andean forest were similar to primary ones with average heights around 10 m and similar mean DBH (15.8 vs 17.3 cm), but lower basal area (12.7 vs $28\text{ m}^2\text{ ha}^{-1}$) and higher stems in the primary site (1082 vs 866) (Aragón et al 2021).

While no field data exists for the selected 1 ha plot polygon in this research, data above shows that while species differ, all species were evergreen, no emergent were present, and structural differences were moderate. EVIs should be comparable.

In order to compare forest type response to climate variables, we geospatially sampled primary forests within 5 km of the secondary forest sites, using the same polygon dimensions and similar topography including elevation, slope and aspect, measured through the Shuttle Radar Topography Mission Digital Elevation Model (SRTM DEM) at 30 m spatial resolution. It is worth noting that the remaining primary forests in San Martín are highly fragmented and, therefore, may have altered ecological characteristics compared to similar montane forests in southern Peru. Primary forest location was determined by using the dry forest map for 2018, for the tropical dry forest, and the Peruvian Amazon forest/non-forest map for the year 2020, for the tropical lowland and tropical montane forests, available through the GeoBosques platform (geobosques.minam.gob.pe) administered by the National Forest Conservation Program to Mitigate Climate Change (PNCBMCC-MINAM) of the Peruvian Ministry of the Environment. Primary forest locations were also visually confirmed using high resolution Sentinel-2 images for the year 2020.

A total of 18 sites were used for this study with 3 secondary and 3 primary forest sites per forest type. See supplementary material table S1 for additional attributes for each plot.

2.2. Landsat data

The EVI has been used to monitor drought impacts on forests (Anderson et al 2018) and is correlated with photosynthetic capacity, leaf area index, canopy structure and morphology (Huete et al 2002). We chose EVI rather than NDVI due to its sensitivity in high biomass areas and NDVI's characteristic of saturating with tropical vegetation (Huete et al 2002). EVI is calculated through the following method:

$$\text{EVI} = 2.5 \frac{\text{NIR} - \text{RED}}{\text{NIR} + \text{RED} - 7.5 \text{BLUE} + 1} \quad (1)$$

where NIR is the near-infrared band, RED is the red band, and BLUE is the blue band. Higher values of EVI indicate higher biomass and greenness (Huete et al 2002) and lower EVI values during or after drought, compared to average, indicate a reduction in productivity and greenness (Caccamo et al 2011). We used Landsat image data from 2001 to 2020 to estimate annual seasonal (i.e. wet and dry season) average EVI from 2001 to 2020 over the secondary forest field sites and primary forest areas of comparison. Landsat imagery has a 30 m spatial resolution (i.e. pixel size), which allows us to record several pixel values within the 1 ha plot area.

LST was derived from top of atmosphere from Landsat's thermal infrared from the Landsat 4–8 collections and available at 30 m spatial resolution. We used Landsat native resolution data from 2001 to 2020 to estimate average wet and dry season LST

from 2001 to 2020. Both EVI and LST data were downloaded from the Climate Engine web application where an automatic cloud and quality mask are applied (app.climateengine.com, Huntington *et al* 2017).

2.3. MODIS data

We used the MODIS (MOD16A2) 8 d, 500 m spatial resolution product to estimate seasonal average ET and potential evapotranspiration (PET) over the secondary forest field sites and primary forest areas of comparison. The available time series included data from 2001 to 2020. In addition, we used the ratio of the MODIS derived ET and PET (ETn), which has been used as a dimensionless indicator of plant water use and is a function of plant water availability and use rather than regional differences in net radiation (Arantes *et al* 2016).

2.4. CHIRPS data

We used the Climate Hazards Group InfraRed Precipitation with Station (CHIRPS) dataset that incorporates weather station data with satellite imagery to provide a more than 35 years of quasi-global, moderate resolution and long temporal precipitation estimates (Funk *et al* 2015). The gridded data set was available at a 4800 m spatial resolution. We used the standardized precipitation index (SPI), derived from the CHIRPS dataset, to estimate local drought anomaly intensity during the wet and dry season of each forest type. The SPI is a widely used drought index, based on accumulated precipitation, to detect precipitation deficits at a specific time scale (McKee *et al* 1993). The wet season is 4 months and the dry season is 8 months for the tropical dry forest. The wet season is 7 months and the dry season is 5 months for both the tropical lowland and montane forests. The SPI scale for drought events (figure 2) include mild dry (below 0 to -0.99), moderately dry (-1.0 to -1.49), severely dry (-1.5 to -1.99), and extremely dry (≤ -2.0) (Naresh *et al* 2009, Svoboda *et al* 2012). Therefore, we used the SPI scale to determine drought conditions during the wet and dry season for each forest type. The average historical year range was chosen for 1981–2020, which is the full record available from the CHIRPS dataset. The CHIRPS, SPI, ET and PET dataset were downloaded from the Climate Engine web application.

All secondary and primary forest plots were located towards the more intact centers of forested area. Mean and standard deviation EVI values, using the native 30 m spatial resolution, for each one hectare plots was used for statistical comparisons between primary and secondary forests and to establish greenness trends. We resampled all variables, using nearest neighbor, to 500 m resolution to have a consistent dataset for correlation and regression

analysis between variables. All data layers and maps were projected in WGS84 UTM Zone 18S. We used ArcGIS Pro 3.0.2 (ESRI) for all geospatial analysis and JASP 0.16.1 (<https://jasp-stats.org/>) for all statistical analysis of the extracted values.

2.5. Data analysis

In order to statistically compare forest canopy greenness in primary to secondary forests for the first hypothesis, we performed a two-tailed Student's *t*-tests, with equal variance, to indicate statistically significant difference between annual and seasonal mean EVI from secondary and primary forests (tables 1 and 2).

Our approach to compare secondary to primary forest vulnerability to drought anomalies, and as a test of the second hypothesis, included the use of one sided Mann–Whitney nonparametric tests to indicate whether there was a statistically significant positive or negative shift of EVI from primary forests compared to secondary forests in response to anomalous drought conditions. Furthermore, to explore the changes in EVI with environmental and climatic variables, we used Pearson's correlation coefficient (*r*) to evaluate the relationship between seasonal mean EVI from 2001 to 2020 and SPI, LST, ET, PET, ETn and year (table 3). Seasonal mean EVI refers to the mean value of EVI for the wet or dry season for each forest type whose length was previously described above. Similarly, we evaluated the relationship between wet and dry season EVI, from 2001 to 2020, with the wet and dry season values of the previous variables (see supplementary material table S2). The normal distribution of the dataset was verified by the Shapiro–Wilk normality test.

Forest canopy greenness differences among the forest types and their differential response to drought anomalies was explored using the two-tailed Student's *t*-tests, as above and as a test of the third hypothesis. In addition, we used stepwise linear regression to first explore the association between mean seasonal EVI and the environmental and climatic variables throughout the length of the study period, from 2001 to 2020. The mean annual EVI was used as the dependent variables, and the environmental and climate factors were selected as independent predictor variables. The statistically significant predictive models use one or multiple variables that best explain the dependent variables. The adjusted R^2 from model fitting indicates the percentage of all factors that explain the pattern of the normally distributed dependent variable. The magnitude of the standardized β indicates the influence of a particular variable in the predictive model. Collinearity diagnostics, from the regression, were used to identify model variables that were highly correlated. We also performed a cross correlation with one to several season time lag intervals between seasonal EVI and the variables.

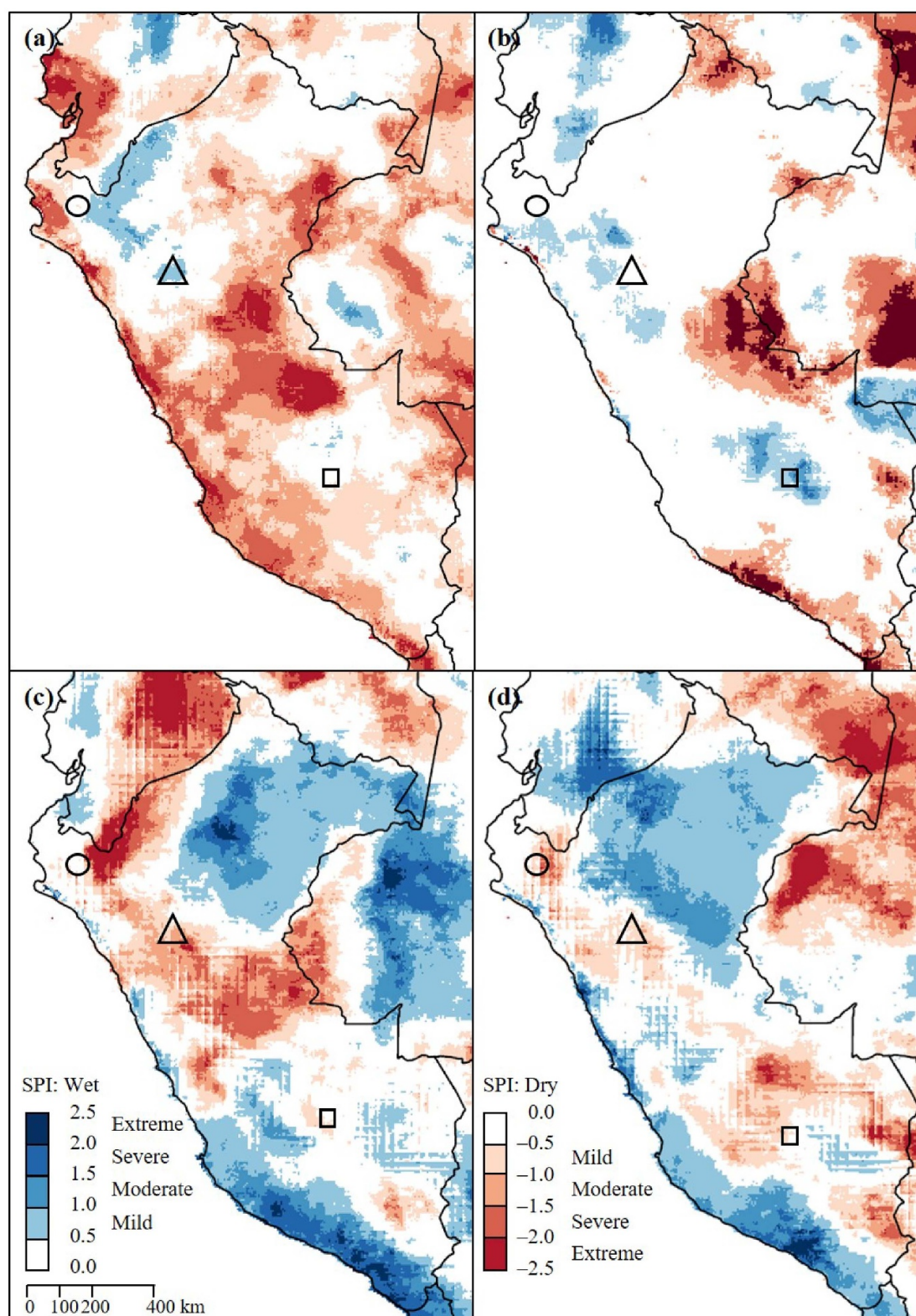


Figure 2. SPI for Peru during the Amazon biome wide drought events of (a) 2005, (b) 2010, (c) 2015–2016 and (d) 2020. Secondary field sites include tropical dry forest (\square), tropical lowland forest (\triangle), and tropical montane forest (\circ).

3. Results

3.1. Forest canopy greenness in primary vs secondary forests in Peru

We found a higher annual and seasonal EVI for secondary forests compared to primary forests with

the 20 years of seasonal data (table 1). Significant differences in EVI were found for mean annual and non-drought anomalies in dry and wet seasons ($p \leq 0.05$). Secondary forests had higher EVI values during seasons with non-drought anomalies compared to primary forests. Primary forests,

Table 1. Mean EVI of secondary (SF) and primary (PF) of Peru between 2001 and 2020. Data are mean (\pm SD) EVI.

	SF	PF
Ave annual	0.50 (0.16)	0.41 (0.16) ^a
Dry season		
Drought	0.42 (0.21)	0.38 (0.17)
Non-drought	0.47 (0.14)	0.35 (0.14) ^a
Wet season		
Drought	0.53 (0.15)	0.51 (0.13)
Non-drought	0.58 (0.10)	0.47 (0.14) ^a

^a Indicates a statistically significant difference between secondary and primary forest EVI value calculated by Student's *t*-test ($p \leq 0.05$).

however, maintained relatively stable and lower EVI levels during the wet season despite wet or drought anomaly conditions. The difference in EVI levels between secondary and primary forests were significant only when water was not a limiting factor (table 1).

3.2. Secondary vs primary forest vulnerability to drought anomalies

EVI of primary lowland forests was higher during anomalous drought events considered moderate to extremely dry ($p \leq 0.05$). However, we also found that EVI was higher in secondary forests compared to primary forests, when precipitation was anomalously high for dry ($p \leq 0.05$) and wet ($p \leq 0.05$) seasons.

Considering these local rainfall deficits and surplus, both secondary and primary forests experienced annual fluctuations in greenness (figure 3), which correlated with plant water use (i.e. ETn, $r = 0.63$, $p \leq 0.001$) and ET ($r = 0.68$, $p \leq 0.001$). During non-drought dry seasons, primary forest productivity was correlated with ET ($r = 0.86$, $p \leq 0.001$), in addition to LST, PET, and ETn ($p \leq 0.001$), which was very similar to secondary forest correlation. Correlations during non-drought wet season was also different, where primary forest productivity was significantly correlated with ET ($r = 0.64$, $p \leq 0.001$), PET ($r = 0.53$, $p \leq 0.001$), and LST ($r = 0.40$, $p \leq 0.001$). Only PET was found to be significantly correlated ($r = 0.29$, $p \leq 0.01$) with secondary forest for those climate conditions.

3.3. Forest canopy greenness differences among forest types and differential response to drought anomalies

Decoupling the response of different forest types, we found a more complex difference of greenness in relation to drought anomalies. Within dry and montane tropical forests, there no significant difference between primary and secondary forest EVI for mild and moderate drought anomalies occurring during

the dry season. In addition, the level of EVI was significantly higher for lowland primary forests compared to secondary forests for mild ($p < 0.05$) and moderate ($p \leq 0.05$) drought anomalies across seasons. No pattern could be found regarding extreme drought anomalies since only a few of these events occurred locally during the years of interest.

Mean seasonal EVI was statistically different for secondary and primary forests, particularly in non-drought wet seasons (table 2), and all seasons for montane forests. In montane forests, mean EVI was consistently higher in all seasonality, which includes drought and non-drought anomalies for the wet and dry seasons, with a low variability between conditions and seasons. However, the montane primary forest had a 62.5% increase in mean EVI value from the average dry season with drought conditions to the average wet season with non-drought conditions. Mean EVI showed a more consistent greening in secondary lowland forests from dry season droughts to normal wet seasons. Under this same climatic condition, secondary dry forests had a 136.0% increase in mean EVI value compared to the relatively stable values in the primary dry forest (table 2).

Correlation analysis between 20 years of seasonal mean EVI indicates a strong positive correlation between mean annual EVI and LST, ET and ETn for both secondary and primary dry forests (see supplementary material table S2). The secondary dry forests had stronger correlation with LST PET and SPI compared to its primary dry forest counterpart (table 3). For montane forests, positive correlations were found between seasonal mean EVI and ETn for both secondary and primary forests ($r > 0.25$, $p \leq 0.01$), and a negative correlation with ET and PET ($r > -0.25$, $p \leq 0.001$) in the primary montane forest (table 3). No cross correlations with different time lag intervals were found between seasonal EVI and the variables.

In stepwise linear regression model fitting for mean seasonal EVI, ETn was the most important parameter that most explained EVI levels for the secondary dry forest ($\beta = 0.693$) and secondary montane forest ($\beta = 0.267$). Secondary dry forests had a negative correlation with LST, which indicates a higher EVI with a lower LST (table 4). Parameter importance and correlation changed with the lowland forests, where a positive trend in mean seasonal EVI over time, in the secondary lowland forest, produced only one model, which contained a statistical correlation with the year of EVI sampled ($\beta = 0.283$, $R^2 = 0.10$, p -value ≤ 0.05) and ET ($\beta = -0.197$).

Model fitting for mean wet season EVI across dry and montane secondary forest sites were mixed with mostly wet season parameters (table 5), with higher

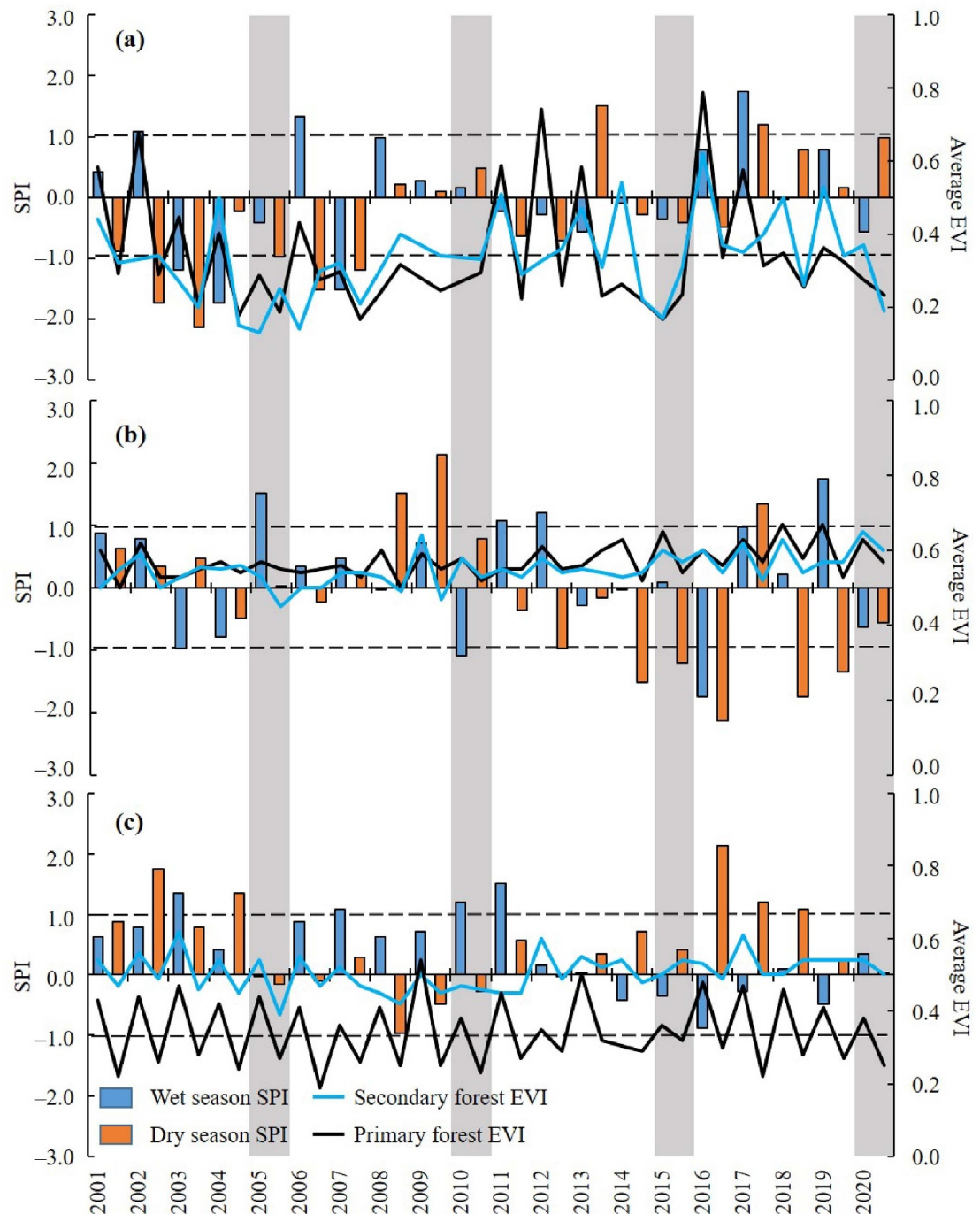


Figure 3. Seasonal SPI, based on data from 1981 to 2020, and average wet and dry season EVI, from 2001 to 2020, over the study sites of (a) TUM I (tropical dry forest), (b) Breo II (tropical lowland forest), and (c) Yanayco (tropical montane forest). Horizontal dashed lines indicate moderately dry (−1.0) and moderately wet (+1.0) lower limits of SPI. Gray bars indicate the Amazon wide drought events of 2005, 2010, 2015–2016 and 2020.

adjusted R^2 for the dry forest ($R^2 \geq 0.44$), compared to the montane ($R^2 \geq 0.29$) and lowland forests ($R^2 \geq 0.13$), indicating that the models for dry forests included at least 44% of the factors affecting wet season EVI values from 2001 to 2020.

4. Discussion

Our study found a clear difference in forest canopy greenness between secondary and primary forests,

where secondary forests had a consistent higher level of greening up, particularly when drought anomalies remained within dry seasons. This level of greenness and leaf growth follows Toledo *et al* (2011) and Poorter *et al* (2016) where tropical successional tree species appear to increase overall biomass growth compared to older successional counterparts. Generally, primary forests maintained the same level of productivity no matter if the wet season experienced rainfall deficit from 2001

Table 2. Mean seasonal EVI, during drought and non-drought anomalies, of secondary (SF) and primary forest (PF) of Peru between 2001 and 2020. Drought anomalies were defined by a negative SPI value. Data are mean (\pm SD). The percent (%) difference considers the difference in mean EVI from drought to non-drought anomalies or as specified from a dry season drought to either a wet season with non-drought or drought anomalous conditions.

	Dry forest		Montane forest		Lowland forest	
	SF	PF	SF	PF	SF	PF
Dry season						
Drought	0.25 (0.05)	0.25 (0.06)	0.47 (0.10)	0.24 (0.05) ^a	0.62 (0.12)	0.57 (0.05)
Non-drought	0.28 (0.04)	0.30 (0.06)	0.53 (0.11)	0.26 (0.06) ^a	0.55 (0.09)	0.55 (0.05)
% diff	12.0	20.0	12.8	8.3	−11.3	−3.5
Wet season						
Drought	0.41 (0.16)	0.36 (0.14)	0.58 (0.06)	0.39 (0.10) ^a	0.63 (0.11)	0.61 (0.06)
Non-drought	0.59 (0.12)	0.42 (0.17) ^a	0.54 (0.08)	0.39 (0.09) ^a	0.63 (0.09)	0.59 (0.05) ^a
% diff	43.9	16.7	−6.9	0.0	0.0	−3.3
Dry season drought to wet season non-drought (% diff)	136.0	68.0	14.9	62.5	1.6	3.5
Dry season drought to wet season drought (% diff)	64.0	44.0	23.4	62.5	1.6	7.0

^a Indicates a statistically significant difference between secondary and primary forest EVI value calculated by Student's *t*-test ($p \leq 0.05$).

Table 3. Pearson's correlation coefficient between seasonal mean EVI of secondary (SF) and primary forests (PF) of Peru, between 2001 and 2020, and predictive variables. Seasonal mean EVI was separated by respective wet and dry seasons for each forest type. Only statistically significant correlations are shown. There were no significant correlations found for year.

Forest site	Temperature	Water availability			SPI
	LST	ET	PET	ETn	
Dry forest					
SF	−0.32 ^c	0.66 ^c	−0.39 ^c	0.72 ^c	0.32 ^c
PF		0.61 ^c		0.59 ^c	
Montane forest					
SF			−0.20 ^a	0.25 ^b	
PF	0.69 ^c	−0.48 ^c	−0.53 ^c	0.26 ^b	
Lowland forest					
SF				−0.18 ^a	
PF	−0.21 ^a				

^a $p \leq 0.05$.

^b $p \leq 0.01$.

^c $p \leq 0.001$.

to 2020. It is important to note that during this time interval, all forests monitored experience at least mild drought for at least 25% of their rainfall seasons, which indicates an important level of persistent water stress and may foreshadow their response.

Despite the increase of canopy greenness of secondary forest after drought conditions, this relationship does not hold when drought anomalies remain during both the dry and wet season, where secondary forests of montane and lowland ecosystems have a lower increase of greenness. This seems to follow the observations of Elias *et al* (2020), which indicates that secondary forests may be more vulnerable to continuous and lengthy drought conditions

that extend beyond typical rainfall seasons. Although prolonged time spans of water stress occurred for no more than 15% of the transitions of dry to wet season for these ecosystems, individual wet and dry seasons with moderate to severe droughts occur and may prevent any consistent increase in productivity.

Decoupling forest type response through predictive modeling, our study found that predicting the magnitude of seasonal greening throughout the length of study period and specifically for the wet season was very similar for both secondary and primary forests, particularly for dry and montane forest types where SPI, LST and ETn were the significant predictor variables. In tropical dry

Table 4. Predictive models of the relationship of seasonal mean EVI of secondary (SF) and primary forests (PF) of Peru, between 2001 and 2020, and predictive variables. Seasonal EVI was separated by respective wet and dry seasons for each forest type.

Forest site	Predictors	Standardized β	R^2	Adj. R^2	p -value
Dry forest					
SF	ETn	0.693	0.66	0.65	a
	LST	−0.323			
	SPI	0.152			
PF	ET	0.550	0.41	0.40	b
	Year	0.245			
Montane forest					
SF	ETn	0.267	0.10	0.10	b
PF	LST	0.618	0.64	0.64	c
	PET	−0.439			
Lowland forest					
SF	Year	0.283	0.10	0.10	a
	ETn	−0.197			
PF	Year	0.269	0.13	0.11	a
	LST	−0.210			
	PET	0.208			

^a $p \leq 0.05$.^b $p \leq 0.01$.^c $p \leq 0.001$.

forest regions, the decrease in LST and the increase of plant water availability would reflect cooler and wetter conditions that would favor greening and, not surprisingly, were strong predictors of EVI changes.

It should be noted that the changes in rain-fall seasonal greening in the secondary and primary forests within the tropical forest biome were predicted by LST in the dry season more than the other factors in our study. LST and EVI have recently been used to improve tropical land cover change classification, as native forests are found to have higher EVI (i.e. canopy cover) with lower LST throughout the year due to the tropical evergreen phenology (Phompila *et al* 2015, Qin *et al* 2019). However, the explanatory factor of LST for lowland secondary forests was not often a predictor as in the primary forest equivalents (see tables 4 and 5). Nevertheless, the extensive historical data of LST over the Amazon biome may be a relatively good predictor of lowland forest greenness changes, offering an unexpected role of temperature over precipitation (Xu *et al* 2015).

Since no time lag correlation was found between mean annual EVI and the predictor variables, the greening response of the forest types apparently occurs sub-seasonally. In other words, greening of tropical dry and montane forests in the wet season is dependent on temperature and water inputs during the same season. In the absence of water limitation, Amazonian forest leaf flush tends to be triggered mainly by insolation increase and secondarily by precipitation increase (Wagner *et al* 2017), which would reflect our predictive models, particularly for

montane primary forests during the wet season, where LST was a strong explanatory factor for seasonal EVI response.

Another important item is that other forest and accompanying ecological characteristics may effect overall forest sensitivity to climate variability. In our study areas, secondary forest sites had similar forest characteristics, similar phenology and some forest composition overlap, but primary forests often had higher tree species diversity. Some secondary forest sites may reach a mature functional diversity but not species diversity, depending on the past logging intensity and level of fragmentation. In addition, shifting and maturing species composition may be more sensitive to climate at different times and particularly to the effects of intense climate anomalies and climate whiplash.

Finally, it is important to note the limitations of using satellite derived data sets and climate models with different spatial resolutions for analysis. The spatial resolution is often quite different where several pixels of data over a 1 ha plot can be extracted and resampled from high resolution images, such as Landsat, while only a very few number of pixels from a coarse resolution climate models may be available, limiting the variability of information, and resampling to a higher resolution may not improve accuracy. Care must be taken when interpreting these results since the heterogeneous effects of drought on the local level may not be represented broad indices such as SPI. Nonetheless, climatic and environmental processes often occur at larger landscapes scales and it is worth attempting to find these correlations to direct future research.

Table 5. Predictive models of the relationship of mean wet and dry season mean EVI for each forest type of secondary (SF) and primary forests (PF) of Peru, between 2001 and 2020, and predictive variables.

Season	Forest site	Predictors	Standardized β	R^2	Adj. R^2	p -value	
Wet	Dry forest						
		SF	LST _w	−0.394	0.48	0.44	b
		ETn _w	0.371				
		SPI _w	0.31				
	PF	SPI _D	0.451	0.35	0.31	a	
		ET _w	0.363				
	Montane forest						
		SF	SPI _D	0.327	0.33	0.29	a
			SPI _w	−0.293			
			ET _w	−0.274			
		ETn _D	0.221				
	PF	LST _w	0.645	0.42	0.41	c	
	Lowland forest						
		SF	Year	0.329	0.15	0.13	a
		PET _D	0.256				
Dry	PF	ET _D	0.364	0.28	0.24	a	
		ETn _w	−0.338				
		Year	0.298				
	Dry forest						
		SF	ETn _D	0.526	0.88	0.87	a
			SPI _w	0.44			
			LST _D	−0.168			
		PET _w	−0.138				
	PF	ET _D	0.915	0.81	0.8	b	
		LST _D	0.486				
LST _w		−0.354					
Montane forest							
	SF	ET _D	0.391	0.15	0.14	b	
PF	LST _D	0.784	0.82	0.8	a		
	SPI _w	−0.318					
	ET _D	0.211					
	SPI _D	−0.196					
	PET _w	0.166					
Lowland forest							
	SF	PET _D	0.298	0.2	0.17	b	
		SPI _D	−0.283				
	PF	LST _w	−0.355	0.21	0.18	a	
ET _D		0.249					

^a $p \leq 0.05$.^b $p \leq 0.01$.^c $p \leq 0.001$.

5. Conclusion

Our study found the overall support of our hypotheses where firstly, secondary forests had higher forest canopy greening overall. Second, we found that secondary forests are more vulnerable to drought anomalies. Lastly, there are differential primary-secondary forest canopy greening and responses to drought anomalies between forest types. Primary forest mostly retained the same level of greening despite water deficits. Changes in LST was a better predictor of forest greening, although this was not always significant in lowland forest sites. The role of temperature as a higher stressor of plant productivity than precipitation has already been mentioned by

other authors (Pechony and Shindell 2010) and represents an extra challenge in a planet where temperature trends and heatwaves are unequivocally increasing (Stevenson *et al* 2022). The use of more than 20 years of historic satellite-based data of optical variables in cloud-based platforms can help identify and forecast forest greening changes, which in turn play key roles on land strategies that target mitigation and adaptation goals to climate change. Thus, secondary forests do not only provide carbon storage but a whole range of other invaluable ecosystem services (Tito *et al* 2022). Additional research is warranted to better understand the response of secondary forests to rapidly changing climatic conditions.

Data availability statement

No new data were created or analyzed in this study.

Acknowledgments

This work was supported by a CONCYTEC (Peru)—World Bank Grant (Contract 011-2019-FONDECYT-BM-INC-INV). In Huayopata, we thank the Cuba and Povea families for their hospitality and help during field work. We thank the collaboration of the Biocorredor Martin Sagrado REDD+ Project with it implementing partners APROBOC, APAHUI, ACOPAGRO and the strategic technical support from PUR. The authors have confirmed that any identifiable participants in this study have given their consent for publication.

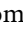
ORCID iDs

Norma Salinas  <https://orcid.org/0000-0001-9941-2109>

Eric G Cosio  <https://orcid.org/0000-0001-6993-5654>

Richard Tito  <https://orcid.org/0000-0002-4184-5654>

Susan Aragón  <https://orcid.org/0000-0002-7364-6094>

Rosa Maria Roman-Cuesta  <https://orcid.org/0000-0002-6945-8402>

References

- Anderson L O, Ribeiro Neto G, Cunha A P, Fonseca M G, Mendes de Moura Y, Dalagnol R, Wagner F H and de Aragão L E O E C 2018 Vulnerability of Amazonian forests to repeated droughts *Phil. Trans. R. Soc. B* **373** 20170411
- Aragón S et al 2021 Aboveground biomass in secondary montane forests in Peru: slow carbon recovery in agroforestry legacies *Glob. Ecol. Conserv.* **28** e01696
- Arantes A E, Ferreira L G and Coe M T 2016 The seasonal carbon and water balances of the Cerrado environment of Brazil: past, present, and future influences of land cover and land use *ISPRS J. Photogramm. Remote Sens.* **117** 66–78
- Brando P M, Goetz S J, Baccini A, Nepstad D C, Beck P S and Christman M C 2010 Seasonal and interannual variability of climate and vegetation indices across the Amazon *Proc. Natl Acad. Sci.* **107** 14685–90
- Caccamo G, Chisholm L A, Bradstock R A and Puotinen M L 2011 Assessing the sensitivity of MODIS to monitor drought in high biomass ecosystems *Remote Sens. Environ.* **115** 2626–39
- Chazdon R L et al 2016 Carbon sequestration potential of second-growth forest regeneration in the Latin American tropics *Sci. Adv.* **2** e1501639
- Costa F R, Schiatti J, Stark S C and Smith M N 2022 The other side of tropical forest drought: do shallow water table regions of Amazonia act as large-scale hydrological refugia from drought? *New Phytol.* **237** 714–33
- Elias F et al 2020 Assessing the growth and climate sensitivity of secondary forests in highly deforested Amazonian landscapes *Ecology* **101** e02954
- Funk C et al 2015 The climate hazards infrared precipitation with stations—a new environmental record for monitoring extremes *Sci. Data* **2** 1–21
- Griscom B W et al 2017 Natural climate solutions *Proc. Natl Acad. Sci.* **114** 11645–50
- Griscom B W et al 2020 National mitigation potential from natural climate solutions in the tropics *Phil. Trans. R. Soc. B* **375** 20190126
- Huete A, Didan K, Miura T, Rodriguez E P, Gao X and Ferreira L G 2002 Overview of the radiometric and biophysical performance of the MODIS vegetation indices *Remote Sens. Environ.* **83** 195–213
- Huntington J L, Hegewisch K C, Daudert B, Morton C G, Abatzoglou J T, McEvoy D J and Erickson T 2017 Climate engine: cloud computing and visualization of climate and remote sensing data for advanced natural resource monitoring and process understanding *Bull. Am. Meteorol. Soc.* **98** 2397–410
- Jiménez-Muñoz J C, Mattar C, Barichivich J, Santamaria-Artigas A, Takahashi K, Malhi Y, Sobrino J A and van der Schrier G 2016 Record-breaking warming and extreme drought in the Amazon rainforest during the course of El Niño 2015–2016 *Sci. Rep.* **6** 1–7
- Jones I L, DeWalt S J, Lopez O R, Bunnefeld L, Pattison Z and Dent D H 2019 Above-and belowground carbon stocks are decoupled in secondary tropical forests and are positively related to forest age and soil nutrients respectively *Sci. Total Environ.* **697** 133987
- Martin P A, Newton A C and Bullock J M 2013 Carbon pools recover more quickly than plant biodiversity in tropical secondary forests *Proc. R. Soc. B* **280** 20132236
- McKee T B, Doesken N J and Kleist J 1993 The relationship of drought frequency and duration to time scales *Proc. 8th Conf. on Applied Climatology* vol 17 pp 179–83
- Nakagawa M et al 2000 Impact of severe drought associated with the 1997–1998 El Niño in a tropical forest in Sarawak J. *Trop. Ecol.* **16** 355–67
- Nareesh Kumar M, Murthy C S, Sesha Sai M V R and Roy P S 2009 On the use of standardized precipitation index (SPI) for drought intensity assessment *Meteorol. Appl.* **16** 381–9
- Paca V H D M, Espinoza-Dávalos G E, Hessels T M, Moreira D M, Comair G F and Bastiaanssen W G 2019 The spatial variability of actual evapotranspiration across the Amazon River Basin based on remote sensing products validated with flux towers *Ecol. Process.* **8** 1–20
- Pechony O and Shindell D T 2010 Driving forces of global wildfires over the past millennium and the forthcoming century *Proc. Natl Acad. Sci.* **107** 19167–70
- Phompila C, Lewis M, Ostendorf B and Clarke K 2015 MODIS EVI and LST temporal response for discrimination of tropical land covers *Remote Sens.* **7** 6026–40
- Poorter L et al 2016 Biomass resilience of neotropical secondary forests *Nature* **530** 211–4
- Potapov P et al 2021 Mapping global forest canopy height through integration of GEDI and Landsat data *Remote Sens. Environ.* **253** 112165
- Qin Y et al 2019 Improved estimates of forest cover and loss in the Brazilian Amazon in 2000–2017 *Nat. Sustain.* **2** 764–72
- Saatchi S, Asefi-Najafabady S, Malhi Y, Aragão L E, Anderson L O, Myneni R B and Nemani R 2013 Persistent effects of a severe drought on Amazonian forest canopy *Proc. Natl Acad. Sci.* **110** 565–70
- Souza R D, Moura V, Paloschi R A, Aguiar R G, Weblar A D and Borma L D 2022 Assessing drought response in the southwestern Amazon forest by remote sensing and *in situ* measurements *Remote Sens.* **14** 1733
- Stevenson S, Coats S, Touma D, Cole J, Lehner F, Fasullo J and Otto-Bliesner B 2022 Twenty-first century hydroclimate: a continually changing baseline, with more frequent extremes *Proc. Natl Acad. Sci.* **119** e2108124119
- Svoboda M, Hayes M and Wood D A 2012 *Standardized Precipitation Index User Guide* (Geneva: World Meteorological Organization)
- Tito R, Salinas N, Cosio E G, Boza-Espinoza T, Muñiz J G, Aragón S, Nina A and Roman-Cuesta R M 2022 Secondary forests in Peru: their differential provision of ecosystem

- services compared to other post-deforestation forest transitions *Ecol. Soc.* **27** [12](#)
- Toledo M *et al* 2011 Climate is a stronger driver of tree and forest growth rates than soil and disturbance *J. Ecol.* **99** [254–64](#)
- Tyukavina A, Hansen M C, Potapov P V, Stehman S V, Smith-Rodriguez K, Okpa C and Aguilar R 2017 Types and rates of forest disturbance in Brazilian Legal Amazon, 2000–2013 *Sci. Adv.* **3** [e1601047](#)
- Wagner F H, Hérault B, Rossi V, Hilker T, Maeda E E, Sanchez A, Lyapustin A I, Galvão L S, Wang Y and Aragão L E 2017 Climate drivers of the Amazon forest greening *PLoS One* **12** [e0180932](#)
- Xu L, Saatchi S S, Yang Y, Myneni R B, Frankenberg C, Chowdhury D and Bi J 2015 Satellite observation of tropical forest seasonality: spatial patterns of carbon exchange in Amazonia *Environ. Res. Lett.* **10** [084005](#)
- Yang Y, Saatchi S S, Xu L, Yu Y, Choi S, Phillips N, Kennedy R, Keller M, Knyazikhin Y and Myneni R B 2018 Post-drought decline of the Amazon carbon sink *Nat. Commun.* **9** [1–9](#)